Quantitative Comparison of Functional MRI and Electro-Cortical Stimulation for Function Mapping

by

Sara E. Larsen

Submitted to the Department of Electrical Engineering and Computer Science
in partial fulfillment of the requirements for the degree of

Master of Science in Computer Science and Engineering

at the

MASSACHUSETTS INSTITUTE OF TECHNOLOGY
[February 2004]
December 2003

Author .....
Department of Electrical Engineering and ~~Com~~puter Science
December 10, 2003

Certified by....
William M. Wells, III
Associate Professor of Radiology, Harvard Medical School
Member of the Faculty of the Harvard-MIT Division of Health Sciences and Technology
Thesis Supervisor

Accepted by .....
Arthur C. Smith
Chairman, Department Committee on Graduate Students

Quantitative Comparison of Functional MRI and Electro-Cortical Stimulation for Function Mapping

by

Sara E. Larsen

Submitted to the Department of Electrical Engineering and Computer Science
on December 10, 2003, in partial fulfillment of the
requirements for the degree of
Master of Science in Computer Science and Engineering

Abstract

Mapping functional areas of the brain is of vital importance for planning tumor resection. An accurate mapping provides information to neurosurgeons about which areas of the brain are *eloquent*, and should be avoided while removing the tumor. With the recent increase in the use of functional MRI for such pre-surgical planning, there is a need to validate that fMRI activation mapping is consistent with the mapping obtained during surgery with the standard technique, direct electro-cortical stimulation. To this end, this thesis quantitatively compares functional MRI mapping with electro-cortical stimulation mapping.

Thesis Supervisor: William M. Wells, III
Title: Associate Professor of Radiology, Harvard Medical School
Member of the Faculty of the Harvard-MIT Division of Health Sciences and Technology

Thesis Supervisor: W. Eric L. Grimson
Title: Bernard Gordon Professor of Medical Engineering

Acknowledgments

I would first like thank my advisor, Dr. William Wells. He has been extremely supportive and encouraging in my research. He has provided advice on my research goals and career goals. He helped me develop my ideas into a really great project. I appreciate everything he has done for me over the past two years.

I would also like to thank Dr. Alex Golby at the Brigham and Women's Department of Neurosurgery. Without her help and support, this project would not have been possible. She has been absolutely amazing to work with, and I value all that she has taught me.

Many thanks to Dr. Ion-Florin Talos for all of his technical support. He spent countless hours segmenting and registering data for this project. Most importantly, he was always available to answer my questions and help me understand the data.

I have had a great experience over the past two years, and I owe this to the interactions I have had at the SPL and at MIT. I would like to thank Dr. Ron Kikinis at the SPL for everything he has done at Brigham and Women's Hospital to make this research possible. I would also like to thank Dr. Eric Grimson for creating such a great research atmosphere at MIT. I have had a wonderful experience working with my fellow researchers and he has made this possible. I would also like to thank him for his personal support of this project.

There are so many of you who have helped me with my research. I would like to thank Corey Kemper and Lauren O'Donnell for helping me understand and sort through the DTI data. I would like to thank Samson Timoner for helping me create awesome meshes. I would also like to thank everyone else in the AI Vision group at MIT for your friendship and support. There is also a whole group of you who helped me figure out stimulation coordinates; many thanks to Steve Hacker, Dan Kacher, Neil Weisenfeld, and Steve Pieper.

I wouldn't have survived my course work at MIT without the support of the 6.1 girls. We stuck together and supported each other academically and socially. I would especially like to thank Laura Miyakawa for her amazing friendship.

I would also like to recognize the great technical support I received from Dave Weinstein at the SCI Institute at the University of Utah. I have had a great experience collaborating with him and look forward to future interaction.

Most of all I would like to thank my family for providing constant support in everything I do. In particular, I would like to thank my older brother, Sam Larsen. He has encouraged me to be my best ever since I can remember. He has provided me with constant advice, support and encouragement. He has had an impact on my life in more ways than he knows. And finally, a huge thanks to my wonderful husband. He has sacrificed so much for me to be here and has supported all of my decisions.

Without all these amazing people in my life, I would not be where I am today. You have all had a large impact on my life. Thank you to everyone. It has been an great adventure.

Contents

List of Figures

List of Tables

Chapter 1

Introduction

1.1 Motivation

Functional magnetic resonance imaging (fMRI) is a non-invasive tool for monitoring brain activity. fMRI measures blood flow changes in the brain in response to a subject performing a task which stimulates particular regions of the brain. These tasks are frequently performed in a block design paradigm consisting of alternating blocks of rest and task; the tasks can include motor, memory, visual or language tasks. Activated areas in the brain require an increase in blood supply in order to facilitate the increase in neuronal activity; this is called the blood oxygenation level dependent (BOLD) effect. The changes in blood supply can be measured with rapid magnetic resonance imaging (MRI).

For several years neuroscientists have used fMRI to study neurological disorders such as Alzheimers, schizophrenia, and multiple sclerosis. Understanding brain dysfunction in such disorders will help lead to treatment and cures. fMRI is also used to help understand healthy brain function and is used to study healthy subjects. Recently, fMRI has become a valuable source of information for neurosurgeons while preparing for tumor resection. Functional area localization provides neurosurgeons with information about the location of eloquent tissue (tissue which is important for the continued quality of life for the patient). There are several risks involved in tumor resection, and better surgical planning improves the probability for success.

Until recently, pre-surgical spatial locations of the tumor and critical functional areas have been mapped based solely on the anatomy of the brain. Anatomical images of the brain provide information about tumor location relative to structure, but they do not provide a functional mapping. Localizing functional areas of the brain provides the surgeon with important information in planning for tumor resection. The current standard for localizing functional areas during surgery is direct electro-cortical stimulation (DECS), whereby the exposed cortex of the patient is stimulated and marked according to patient response, a processes that provides a mapping of functional regions on the cortical surface. For instance, during surgery, after the craniotomy, the neurosurgeon stimulates the surface of the cortex in regions around the tumor with a bipolar stimulator injecting current pulses. The awake patient is able to communicate with the surgeon and perform tasks evoking regions near the tumor. In this context, the stimulation is an inactivation method stimulating what would happen if that region of the brain were damaged during surgery. If the stimulation causes inhibition of the patient's task, this region is deemed eloquent and be avoided during resection. Several stimulation sites are tested and a mapping of labeled tags on the brain surface provides the neurosurgeon with a functional mapping. This functional mapping provides the surgeon with valuable information when planning for tumor resection. Figure 1-1 shows a photograph taken during surgery of the labeled tags marking stimulation sites. Such a mapping is accompanied with annotations indicating patient response at each stimulation site.

Direct electro-cortical stimulation is stressful for the patient and in some cases cannot be performed. This is especially true for children. There is a substantial effort on the part of scientists and neurosurgeons to improve the techniques used to map tumor and functional area locations, particularly by the usage of fMRI. fMRI techniques provide a non-invasive means for functional mapping and can be performed before the surgery. However, there is a need to validate that fMRI data does represent an accurate mapping of function in the brain. The goal of this thesis is to address the problem of validating fMRI for surgical planning.

fMRI activation maps provide a functional mapping that can be used to plan

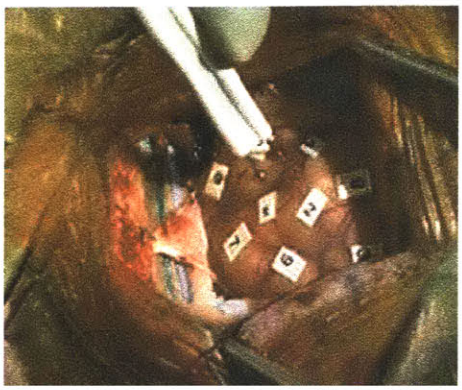

Figure 1-1: Photograph of the cortical surface with labels tags indicating stimulation sites.

for tumor resection. Figure 1-2 shows a superior view of a human brain model and a model of fMRI activation regions. The fMRI activation regions are indicated in purple and the tumor is indicated in green. The regions are activated in response to the subject performing a hand motor task. Knowing the location of activating regions relative to tumor location is of vital importance in surgical planning. Since tissue damage in these regions should be avoided. This information can be used in planning how to remove the tumor.

With the recent increase in the use of fMRI for pre-surgical planning, it is important to use DECS to establish the utility of fMRI for accurate localization of eloquent brain regions. To our knowledge all previous research has performed a qualitative comparison of functional mapping methods. It is clear that there is a crucial missing link in the previous research that we aim to address – a quantitative validation through statistical comparisons of spatial information.

Many sites have reported problems and sources of error that arise in trying to evaluate the agreement of the two modalities [10, 14]. One such problem in evaluating the agreement of DECS and fMRI data is determining how to compare the voluntary movement performed during the fMRI scan to the involuntary (either inhibitory or induced) effect caused by electro-cortical stimulation [14]. Additionally, stimulation within the depth of a sulcus is not normally performed [14], and therefore a large portion of the cortex cannot be stimulated, resulting in an incomplete cortical

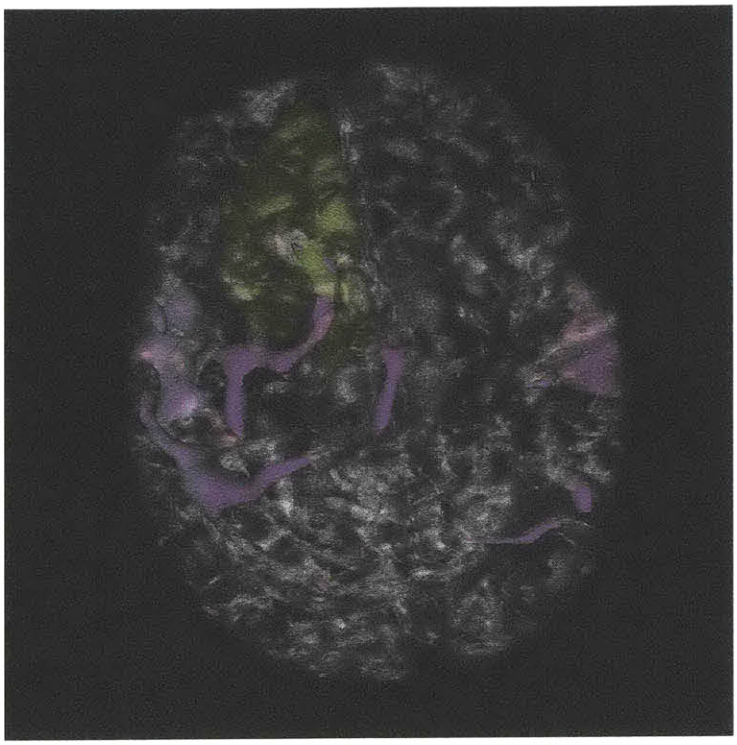

Figure 1-2: Superior view of human brain. The fMRI activation regions are indicated in purple and the tumor is indicated in green.

mapping.

1.2 Contributions

This thesis aims to validate fMRI for pre-surgical functional mapping. Providing surgeons with more information will help them plan for tumor resections. We have contributed to the validation of fMRI by developing a method for quantitative comparison of fMRI and DECS functional mapping techniques. Our methods integrate existing technologies to achieve this comparison, including registration of multimodal image sets and segmentation of the brain, tumor, and ventricles [35]. We also use existing meshing techniques [27], and existing finite element method solving software [22]. Our contributions bring these technologies together to help surgeons validate fMRI for pre-surgical planning.

We built a patient-specific brain conductance model that is used to simulate the

DECS mapping procedure. DECS data taken during surgery consists of stimulation coordinates and patient response at each stimulation site. This data is used as input parameters in solving for the three-dimensional current density distribution due to cortical surface stimulation. The current density distribution is a representation of the complete DECS mapping. This DECS stimulation map is compared with the fMRI activation map using the Dice similarity coefficient as a measure of overlap between the two volumes.

We used structural MRI along with diffusion tensor imaging (DTI) to build a patient-specific electrical model of the brain that is used to solve for the current density distribution. Additionally, patient specific conductivity tensors are computed and used to model tissue anisotropy in electrical conductivity. The electrical conductivity tensor is computed using a direct linear relationship to the diffusion tensor [28].

The improvements we have made include the use of a patient-specific conductivity tensor model to find the current density distribution. This provides a complete mapping of DECS methods. Additionally, we demonstrate a method to quantitatively compare the DECS stimulation and fMRI activation maps using Dice similarity coefficients [4] and variable thresholds to achieve a maximal Dice similarity measure.

The final goal is to validate the utility of fMRI for pre-surgical planning. The use of fMRI along with accurate conductivity models could lead to less injury to eloquent brain areas during surgery and a more ambitious approach to tumor removal.

1.3 Organization of Thesis Document

This thesis presents a method for performing a quantitative comparison of fMRI and DECS functional mapping methods. A brief background on related work at other sites is discussed in Chapter 2. Clinical materials and methods, including imaging modalities and surgical setup, is discussed in Chapter 3. Details describing the DECS stimulation map are explained in Chapter 4. Results are reported in Chapter 5, and Conclusions are drawn in Chapter 6.

Chapter 2

Background

Validation of fMRI with electro-cortical stimulation methods is active research at several sites [5, 10, 12, 14, 18, 19, 21, 34, 36]. A better understanding of the information provided by fMRI will lead to its validation and use in preparing for tumor resection. In this chapter, different stimulation methods will be presented. Additionally, field solving methods will be described. Previous work will be described, and finally, comparison difficulties will be discussed.

2.1 DECS Methods

There are several functional mapping methods used during surgery [3]. These methods use stimulation and recording electrodes to map functional areas of the cortex. Simple functional mapping may be accomplished using intra-operative direct electro-cortical stimulation (DECS). This mapping is done by stimulating the surface of the brain with a bipolar stimulator, which injects current pulses at a frequency of 5-75Hz and an amplitude of 2-10mA. When mapping functional areas using DECS, the patient usually remains awake during stimulation. When mapping the motor areas, the patient communicates any muscular tingling or twitching to the surgeon while the cortex is stimulated. To map the language areas, the patient must perform tasks such as counting or naming. Stimulation mimics brain lesions, and an inability to perform these tasks provides information about which regions are eloquent.

Recording electrode arrays are often used during stimulation to record current spread and neuronal response. This can provide the surgeon with knowledge about how the current travels through the cortex. Electrodes recording high neuronal activity in response to nearby stimulation could indicate connectivity between the stimulation and recording sites. The use of depth electrodes are also used in surgical cases for functional mapping. Depth electrodes are used to record from within the cortex around stimulation sites [30]. Depth electrodes also provide information about neuronal response, but they have the ability to record from within the cortical surface, providing information about the response within cortical layers.

2.2 Previous Work

2.2.1 Field Solving Methods

Biological systems send messages via electrical signals. Understanding how these signals propagate through such systems will lead to a better understanding of how these systems function [31]. In our case, better understanding of how the brain sends electrical information will provide more information in planning for tumor resection. Field solving shows how injected currents travel through the brain using conductivity models. Field solving in biological systems is an active area of research, particularly as applied to source localization problems. Electrophysiological methods such as electroencephalography (EEG) and magnetoencephalography (MEG) are based on mapping the source of neuronal activity by measuring voltages outside of the head. In such problems, current sources in the brain are modeled as current dipoles which have two components: a primary current representing the source of neuronal activity, and a secondary current which is a volume current resulting from the interaction of the primary current with the conductive tissue in the brain [29]. Closed form solutions can be found by modeling the brain as concentric spheres. However, when using a geometrically realistic brain model, approximation methods must be used. Common methods include finite element methods and boundary element methods. In work

done by Van Uitert *et al* [29] a simulation of source localization for MEG forward and inverse solving is described. They compare the results when using spherical brain models and realistic models. Wolters *et al* [1] used a realistic brain model and incorporated tissue conductivity inhomogeneities and anisotropies into solving for EEG and MEG source localization. They show that their finite element modeling methods are stable when using realistic brain models with tissue anisotropy. In the work by Tuch *et al.* [9] tissue anisotropy was determined using diffusion tensor data to estimate the conductivity tensors of the brain model. They used a realistic model with conductivity tensors to solve MEG and EEG source localization problems.

2.2.2 fMRI and Electro-Cortical Stimulation Comparison

Several sites [5, 18, 34] performed comparison studies of fMRI and electro-cortical stimulation mapping methods. These sites use rendered fMRI activation maps that are compared to an intra-operative photograph of the cortex indicating stimulation sites with labels on the cortical surface. Such an image is shown in Figure 1-1. The labels are annotated with the recorded response. Puce *et al.* [18] used an array grid to record from the cortical surface. Both Yetkin, *et al.* [34], and FitzGerald *et al.* [5] used patient response to stimulation to annotate the cortical tags. The fMRI activation map was registered to the intra-operative photograph using anatomical landmarks. Comparison studies were performed by qualitatively measuring the amount of overlap in activated regions with stimulation sites that indicated a positive response. The results are reported as overlap or no overlap. These sites report "good agreement" and indicate that their findings support fMRI for functional mapping.

Krings *et al.* [14] compare fMRI activation maps to several functional mapping modalities in order to map motor functional areas. These include positron emission tomography (PET), transcranial magnetic stimulation (TMS), and direct electro-cortical stimulation (DECS). In their DECS experiments, the cortex is stimulated using a $1cm^2$ silver place electrode. Compound muscle action potentials (CMAP) are recorded using subcutaneaous needle electrodes inserted into the lower and upper limbs. If the recorded CMAP reached a predetermined threshold, the corresponding

stimulation site was marked accordingly. Stimulation coordinates were obtained using a steroe-tactic navigation device and marked within the three dimensional MRI data set. The distance was measured between the fMRI activation regions and stimulation sites that reported recordable CMAP's. This experiment shows no contradictory results in comparing fMRI and DECS (measured distance $>2cm$), and most experiments show overlapping results.

In the work by Hill *et al.* [10], eight patients with epilepsy underwent intraoperative stimulation using a subdural electrode mat consisting of 64 electrodes. Activated voxels from the three dimensional fMRI activation map were compared with the location of the electrodes that elicited sensory response in the patients. The distance between each electrode and the center of the activated region from the fMRI activation map was measured. After motion and brain deformation corrections, they report good agreement between the two mapping modalities. However, they report that brain deformation makes it difficult to draw a qualitative conclusion about the ability of fMRI to provide the same information that DECS provides and conclude that fMRI is unsatisfactory for localization of functional regions in patients with epilepsy.

2.3 Inconsistencies in Comparing fMRI and DECS

Functional mapping for tumor resection consists of mapping functional areas near and around the tumor and craniotomy. Functional mapping by way of DECS allows the neurosurgeon to choose stimulation sites. In contrast, pre-surgical functional mapping by way of fMRI is accomplished by choosing paradigms that will activate regions near the tumor and proposed craniotomy opening.

There is an inherent mismatch in comparing fMRI activation methods to electrocortical mapping methods. fMRI measures the blood flow changes in response to tasks that are voluntarily performed by the subject and it is therefore an activation method. Activated regions within the fMRI map indicate that *all* voxels within a region were activated in response to the task performed. In contrast, DECS mimics

what would happen if a particular part of the brain were damaged and how it would affect function. It is therefore a deactivation method. DECS stimulation sites that evoke patient response indicate that *some* of the tissue within the region of stimulation was activated and caused deficit in the patient, but it does not indicate that the entire region was responsible for the deficit. Despite these differences, several surgeons believe there is some physiological agreement between these functional mapping methods.

2.4 Sources of Error

In addition to the inherent mismatch in comparing DECS and fMRI mapping methods, there are technical problems that make the comparison difficult. These sources of error include motion artifacts and registration inaccuracies. Previous research provides inconclusive results as to whether or not fMRI should be used in planning for tumor resection.

Hill, *et al.* provide an extensive survey of previous research. They describe the sources of error that lead to the conclusion that not enough research has been performed to deem fMRI the best method of functional localization for surgical planning. First of all, there are several registration errors in performing a comparison study between fMRI and electro-cortical techniques. Registration errors arise in motion of the subject during scan time. Motion correction algorithms are frequently used to help fix this error. Another source of registration error comes from brain deformation due to the craniotomy and tumor resection. When the cranium is removed, the brain sinks slightly. Registering intra-operative MRI scans to pre-operative MRI scans require non-rigid registration algorithms to be most effective.

Chapter 3

Clinical Materials and Methods

This chapter describes the clinical methods used for obtaining patient-specific data. The anatomical MRI data and the diffusion tensor data are used to construct the patient-specific conductivity model. The DECS intra-operative stimulation coordinates and patient response are used as model parameters to find the current magnitude distribution at each stimulation site. Finally, the the DECS stimulation map is compared to functional MRI activation map.

Comparison of DECS and fMRI mapping techniques were performed retrospectively on data collected from a neurosurgical case (collected under informed consent). The patient suffered from complex partial, secondarily generalized seizure. The patient had some word finding and other expressive language difficulties. The tumor was a large diffuse astrocytoma involving the frontal and temporal lobes in the dominant (left) hemisphere - the hemisphere responsible for language function. A subtotal neurosurgical resection was performed in an intra-operative MRI scanner via a fronto-temporal craniotomy with awake language mapping using cortical bipolar stimulation. The patient noted slight cognitive improvement post-operatively. The tumor resection was limited by involvement with key language cortex and underlying white matter tracts.

Several pre-operative images were taken of the patient including high resolution MRI, diffusion tensor imaging (DTI) and fMRI. The details of the data collection are described below.

3.1 Anatomical Description of the Brain

Anatomical magnetic resonance imaging (MRI) provides information about brain structure and anatomy. Most MRI scanners use super conducting coils to induce a magnetic field strong enough to align the nuclear spin of many atoms. The most prominent atom in the human body is hydrogen [32]. The nucleus of the hydrogen atom behaves like a magnetic dipole; when a magnetic field is applied, the spins either align against or with the magnetic field depending on the energy state of the atom. A hydrogen atom has two states; when it is in a low state the atom is aligned with the magnetic field. When the energy state is high, the atom is aligned against the magnetic field. A change in energy state is accompanied by absorption or emission of energy in the radio frequency range. Radio frequency pulses are used to encourage the nucleus to change energy states. This changing of states can be detected by radio frequency emissions, providing information about the material being imaged [32]. Suprisingly enough, this technology can be used to obtain high resolution volumetric images of anatomy.

The patient underwent two pre-operative anatomical imaging protocols: (1) a whole brain axial 3D-SPGR (slice thickness=1.5mm, TE/TR=6/35$msec$, FA=75°, FOV=24cm, matrix=256x256); (2) an axial T2-weighted fast-spin-echo (slice thickness =5mm, TE/TR=100/3000$msec$, FOV=24cm, matrix=256x192). Brain and ventricular system segmentations were obtained from the 3D-SPGR, using a curved surface evolution algorithm [35]. The tumor was manually segmented using the T2-FSE images, which provide high tumor contrast. The 3D models were built using the label maps generated from the segmentation. Figure 3-1a shows pre-operative 3D-SPGR image slices at the three intersecting planes, and Figure 3-1b shows the corresponding brain segmentation imposed on the pre-operative 3D-SPGR images. Using the segmented label maps, models of the brain, tumor and ventricles were built in the 3D-Slicer [24, 7]. 3D-Slicer using a marching cubes algorithm and a Gaussian smoothing algorithm to generate smooth surface models.

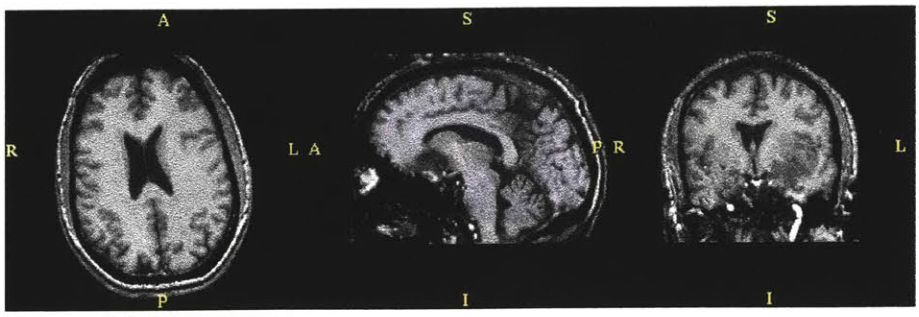

(a) Pre-operative 3D-SPGR images of intersecting planes.

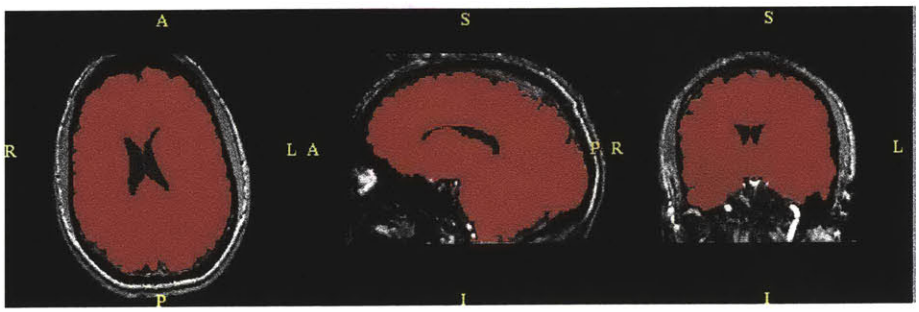

(b) Corresponding brain segmentation (pink) imposed on pre-operative 3D-SPGR.

Figure 3-1: Brain segmentation using pre-operative 3D-SPGR.

3.2 Diffusion Tensor Imaging

Diffusion tensor imaging (DTI) provides information about location, direction and extent of white matter tracts [26]. To accomplish this, DTI uses MRI detection of water molecule motion in tissue. In highly structured tissue, water molecules have less restricted movement in the direction of the fibers making up the tissue; in white matter the water molecules move along the myelinated axons. The diffusion of water within a voxel can be represented with a tensor. The tensor is represented as three orthogonal eigenvectors and their corresponding eigenvalues [26]. The diffusion tensor represents the probability of movement in any direction. Figure 3-2a is an illustration showing how the diffusion of water is higher in the direction of the axon fibers. Figure 3-2b shows how this diffusion can be described using a tensor, which corresponds to an ellipsoid in three dimensions.

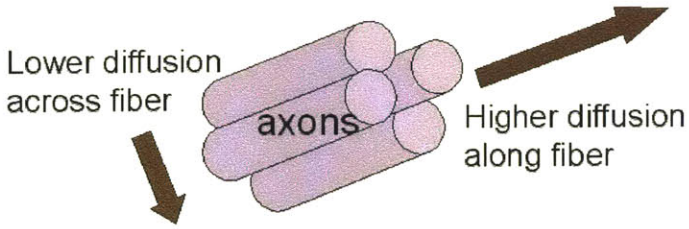

(a) Diffusion of water is higher along direction of axon fibers than it is across axon fibers.

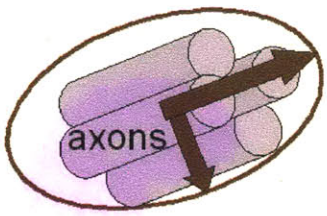

(b) Tensors are used to describe diffusion of water, which correspond to an ellipsoid.

Figure 3-2: Illustration of diffusion tensor.

Diffusion tensor images (axial line scan diffusion images (LSDI) [8]) (TE=64$msec$, TR=2592$msec$, slice thickness=4mm, slice gap=1mm) were obtained covering the region of interest. The 3D tractography method used is described by [33], which is fully implemented in 3D-Slicer. White fiber tracts are found by tracking the direction of the principle eigenvector [26]. The baseline acquisition of the LSDI was used to register to the 3D-SPGR data set. The registration was performed manually by experienced neurosurgeons at Brigham and Women's Hospital.

Diffusion tensor data can be displayed in 3D-Slicer. In 3D-Slicer, the tensors are displayed as glyphs overlayed on the gray-scale image. The length of the glyph corresponds to the largest eigenvalue, and the direction corresponds to the principle eigenvector. The color corresponds to the degree of anisotropy [13]. Figure 3-3 shows an example of diffusion tensors using glyph visualization.

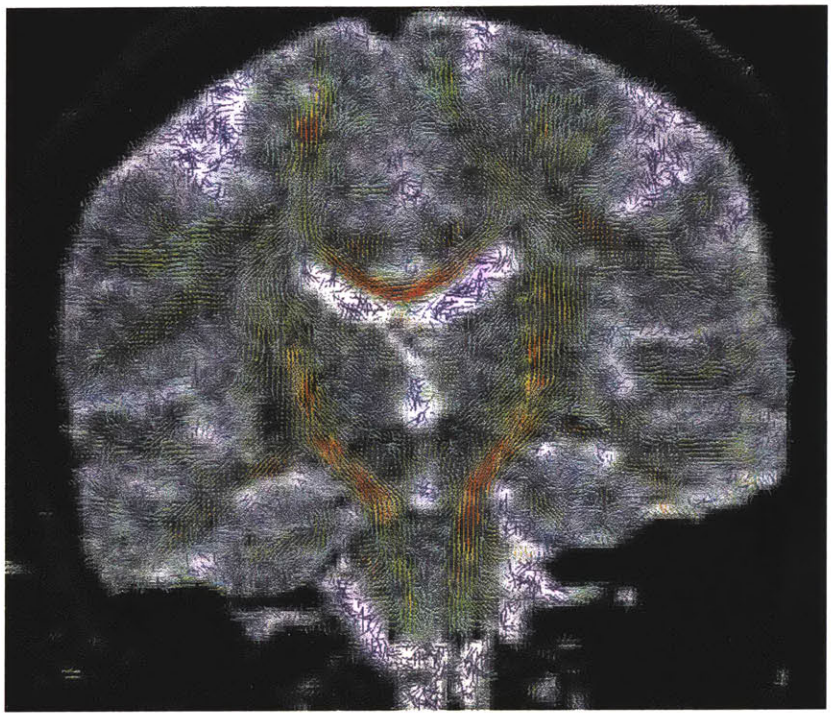

Figure 3-3: Visualization of the tensor data is shown as 3D glyphs corresponding the magnitude and direction of the diffusion at each voxel. Regions of high anisotropy, such as the corpus callosum and corticospinal tract, are in red.

3.3 Surgery

Surgery was performed in the MR Therapy (MRT) [20] at the Brigham and Women's Hospital. The MRT is an open magnet MRI scanner that allows intra-operative scans to be taken during surgery. Figure 3-4 shows the surgical setup in the MRT.

Figure 3-4: Surgical setup in the MRT at Brigham's and Women's Hospital.

The MRT operating room provides the surgeons with updated images of patient anatomy. Additionally, the intra-operative images are used to integrate pre-operative data into the operating room via registration of pre-operative 3D-SPGR with intra-operative 3D-SPGR. Figure 3-5 shows pre-operative models of the ventricles, tumor, and white matter tracts registered to the intra-operative 3D-SPGR data.

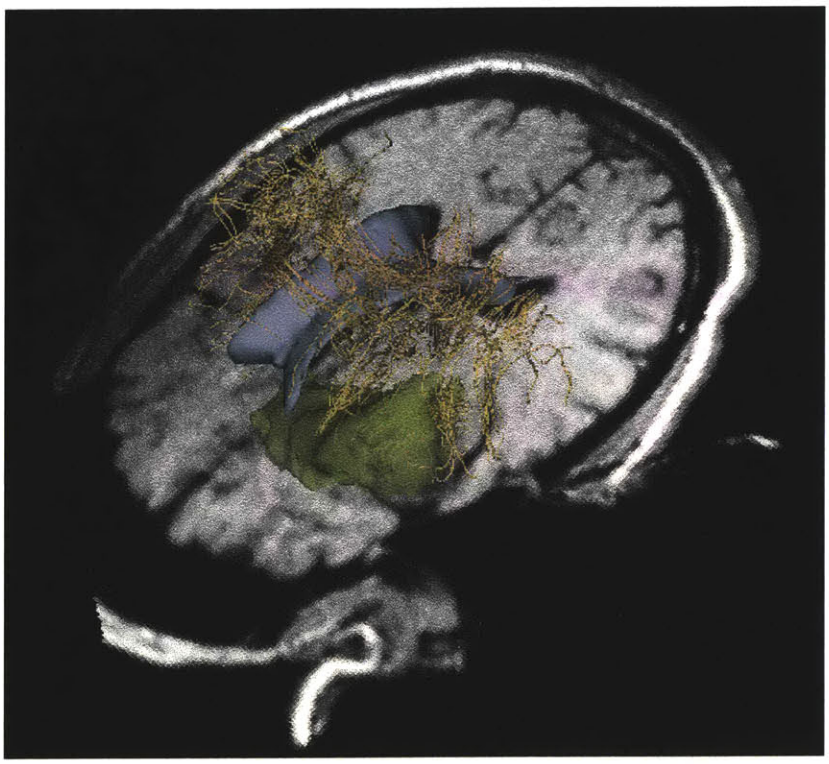

Figure 3-5: Pre-operative models of the ventricles (blue), white matter tracts (yellow) and tumor (green) registered to the intra-operative 3D-SPGR images.

3.4 Direct-Electro Cortical Stimulation Procedures

During surgery, after the craniotomy and before tumor resection, functional mapping of the language areas by way of DECS was performed. The exposed cortex of the patient was stimulated with an Ojemann bipolar stimulator with $2mm$ diameter ball contacts separated by $5mm$, [16]. The stimulator is shown in Figure 3-6. The stimulator injects current pulses at 5-75Hz at an amplitude of 2-10mA. The surgeon stimulated the cortex at seven sites while the patient either counted to ten, or listed the days of the week. The stimulation sites were marked with labeled tags and annotated according to patient response. After the DECS mapping was performed, the surgeon located each site with a sterotactic navigation probe. The intra-operative coordinates of the probe tip were read from the locator workstation in the coordinate system of the intra-operative images. Registration of the stimulation coordinates to the conductivity model is a straightforward application of the transformation between

intra-operative 3D-SPGR and pre-operative 3D-SPGR. Figure 3-7 shows the location of the stimulation coordinates.

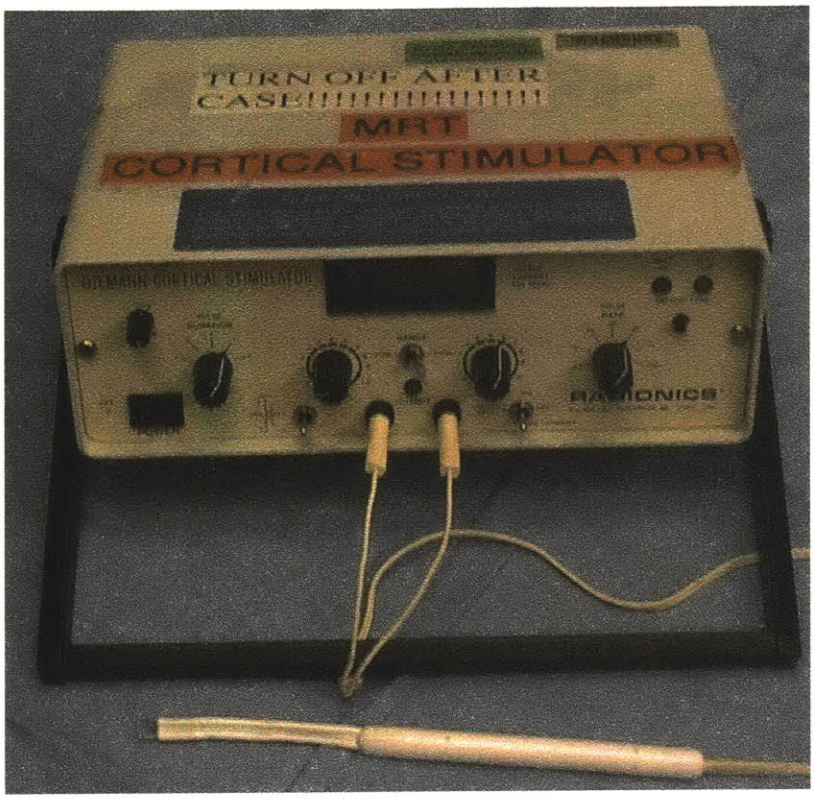

Figure 3-6: Radionics Bipolar Ojemann stimulator

3.5 Functional Mapping

Functional MRI (fMRI) uses rapid MRI imaging techniques to obtain information about blood flow changes in the brain. These blood flow changes are in response to increased energy utilization within activated regions [11]. Brain regions are activated by performing tasks while the MRI volumes are taken over time. fMRI task protocols often use a block design paradigm where rest and task timing is governed by a block design as shown in Figure 3-8a.

Since image volumes are taken every few seconds, some image volumes will be taken at rest and some will be taken while the patient is performing the specified task. Parts of the images taken during stimulation will have increased intensity

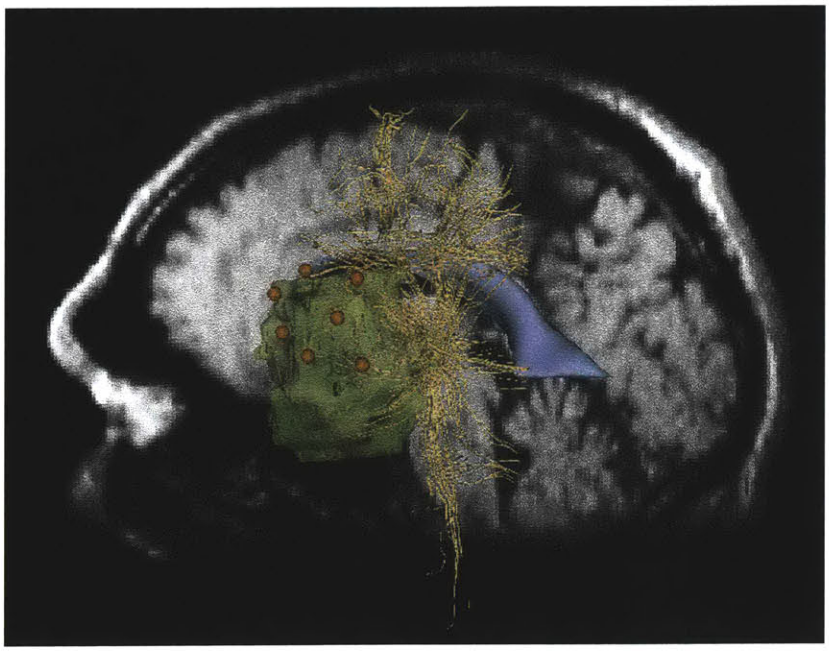

Figure 3-7: Stimulation sites (orange) registered to pre-operative 3D-SPGR images. Tumor (green), ventricles (blue) and white fiber tracts (yellow) are also shown.

compared to those taken during rest. This is due to the BOLD effect, discussed in Chapter 1. These regions with increased intensity should correspond to regions in the brain which are activated by the task [11]. Figure 3-8b shows the intensity of an activated voxel traced through all volumes in the series.

fMRI analysis detects these activated regions within the fMRI dataset. There are several ways to detect activated regions, and this detection is an active area of research. A simple approach correlates the time-series of each voxel with the block design protocol. If a voxel's time-series has high correlation with the protocol, then it is likely that the region is activated.

For our detection we used SPM99 [25], which uses the general linear model (GLM) [6]. The GLM sets up a pattern that is expected in the data. The data is then fit to this pattern. A simple linear model for one voxel is shown below:

$$y(t) = \beta * x(t) + e(t),$$

Where $y(t)$ is the time-series data at one voxel, β is the parameter estimate (PE),

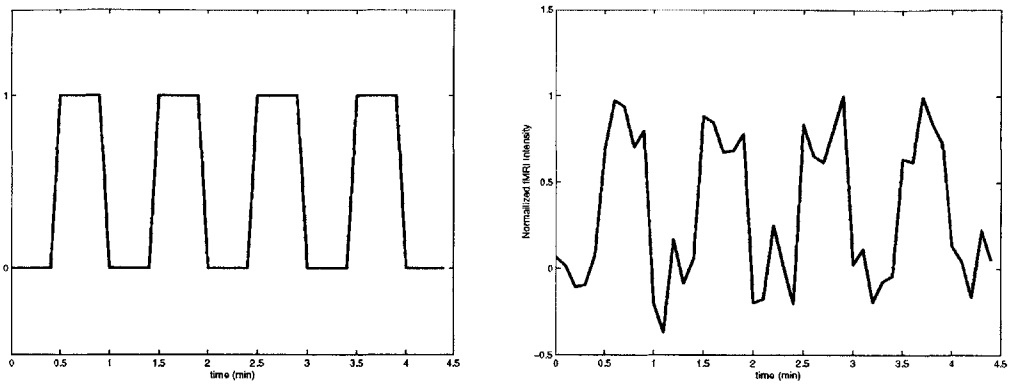

(a) fMRI design protocol; zero corresponds to rest and one corresponds to task.

(b) fMRI time-series for an activated voxel.

Figure 3-8: fMRI design protocol and activation response at one voxel.

$x(t)$ is the block design protocol, and $e(t)$ is the error. The parameter estimate is the value by which the square wave by which the protocol must be multiplied in order to fit to the data time-series. The model fitting involves adjusting this parameter to find the best fit. The error term, $e(t)$, allows for fitting errors.

The parameter estimate can be used to compute statistical significance on whether or not a voxel was activated. Frequently, the T-statistic is used; it is computed as follows:

$$T = \frac{\hat{\beta}}{\text{standard error}(\hat{\beta})}.$$

The T-statistics are now thresholded by determining a value at a given level of significance. The thresholded T-statistics provide a binary fMRI activation map where all voxels with values above the threshold are one and all other voxels are zero.

Whole head fMRI image volumes were obtained (TR/TE=2000/50$msec$, FA=90^o, FOV=24cm, matrix=64x64, voxel size= 3.75 x 3.75 x 4 mm^3). The language areas were mapped using a processing task that tested the patient's level of semantic versus perceptual judgment. The subject was shown 24-second blocks of either a fixation cross or words (6 words presented for 4 seconds each). For the cross, the subject was

told to focus on the cross. For the words, the subject was told to press a button if 1) the word was written in capital letters (i.e. FAME), or 2) if the word was concrete (i.e. rock). These tasks tested 1) perceptual decision tasks, and 2) semantic decision tasks. Instructions were given visually for 4 seconds prior to each block of words and told the patient which decision should be made.

SPM99 was used for reconstruction and motion correction of the data. SPM99 was also used to calculate voxel by voxel paired T-statistic scores for each voxel. Thresholded scores were then used to generate a binary fMRI activation map. This map was used to generate a 3D model using 3D-Slicer [24].

Figure 3-9 shows an example of fMRI activation regions for a series of coronal slices. The fMRI activation map is imposed on 3D-SPGR image slices.

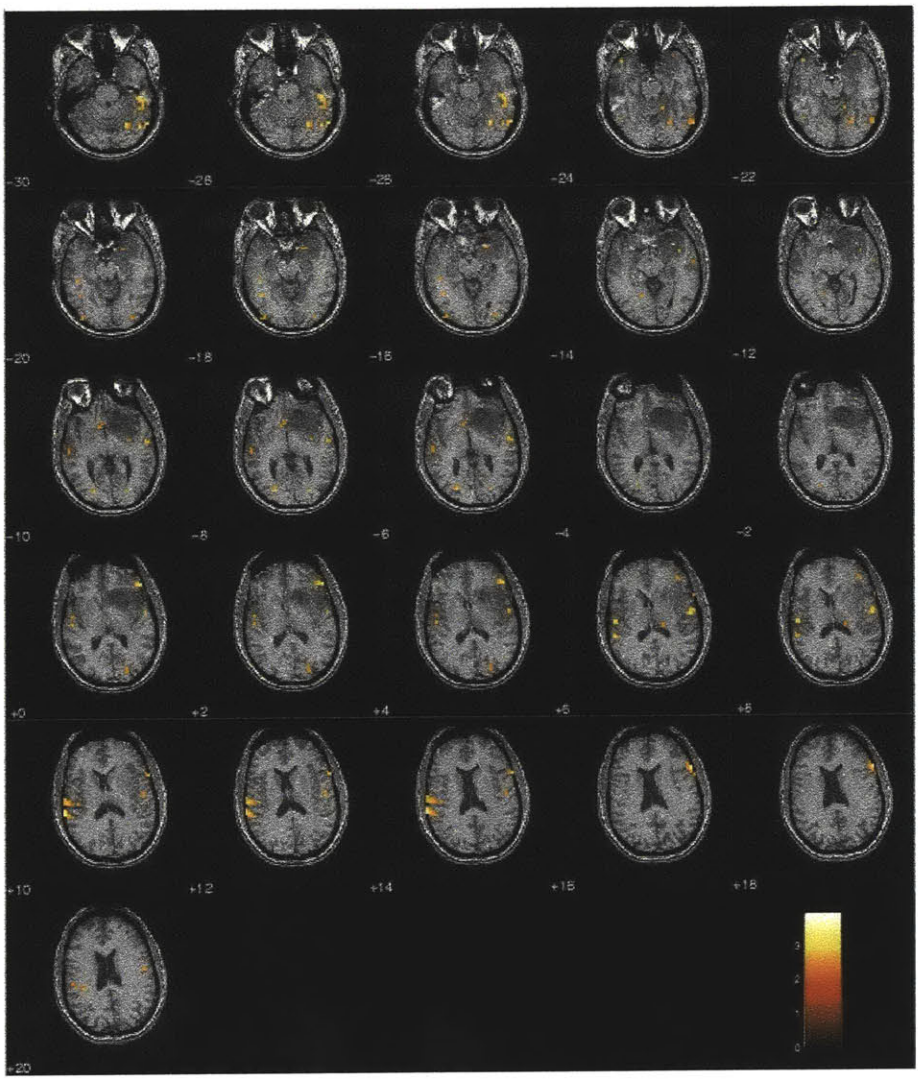

Figure 3-9: fMRI activation regions imposed on 3D-SPGR image slices.

Chapter 4

DECS Stimulation Map: Computational Methods

In this chapter we describe the computational methods for building the patient-specific conductivity model and show how it is used to compute the direct electro-cortical stimulation (DECS) stimulation map. The model contains information about the electrical properties of the tissue and can be used to solve for the current density distribution in response to current injected on the cortical surface. The current density solution shows how current travels through the tissue and therefore which regions are activated by the stimulation; this is the DECS stimulation map. The map is a three dimensional volume of scalar values indicating current density magnitude. This current density is determined by solving the quasi-static boundary-value problem governed by Poisson's equation. In order to compute this map, a high resolution description of the anatomy is needed. This anatomical description is represented using a mesh of tetrahedral elements. For each tetrahedra element, the corresponding conductivity tensor is determined by a direct linear relationship to the diffusion tensor [28]. The conductivity tensor models tissue anisotropy in the brain. The partial differential equations governed by Poisson's equation can then be solved using the finite element method. The patient-specific conductivity model is used to solve for the current density distribution due to direct electro-cortical stimulation. Finally, this chapter describes the methods for obtaining this DECS stimulation map.

4.1 Model Geometry

The brain geometry is obtained using the 3D-SPGR data, which provides a high resolution anatomical description. Using a curved surface evolution algorithm [35], the brain is isolated from the skull. This data provides information about brain boundary, shape, and structure. The resulting segmentation consists of a binary label map describing which voxels are brain and which are background.

Based on the segmentation, a tetrahedral mesh was constructed for use in finding the electric field solution using the finite element method. Tetrahedral elements are a simple three dimensional volume element. They are particularly useful in that they can be used to accurately describe smooth surfaces [27]. To form the mesh, an oct-tree method is used whereby the volume is filled with cubes and then subdivided into tetrahedral elements. The brain surface is fit by intersecting the edges of the mesh with the surface of the volume. This intersection is found by checking for edges in which one end lies inside the brain and the other in the background. These edges are subdivided and new tetrahedra formed so that the tetrahedra conform to the surface as described in [27]. The mesh used in this experiment has tetrahedral elements on the order of $5mm^3$. Figure 4-1 shows the surface boundary of the tetrahedral mesh.

4.2 Conductivity Tensors

Now that the brain geometry is described using tetrahedral elements, anisotropic conductivity tensors are assigned to each element. The conductivity tensors can be directly computed from the diffusion tensor [28]. Tuch *et al.* modeled the relationship between the conductivity and diffusion tensor by relating these transport tensors through the statistics of the medium microstructure [28, 23]. The relationship between the conductivity and diffusion tensors was fit and found to be a linear scaling of the eigenvalues. The linear model is described below:

$$\sigma_\nu = k(d_\nu - d_\varepsilon).$$

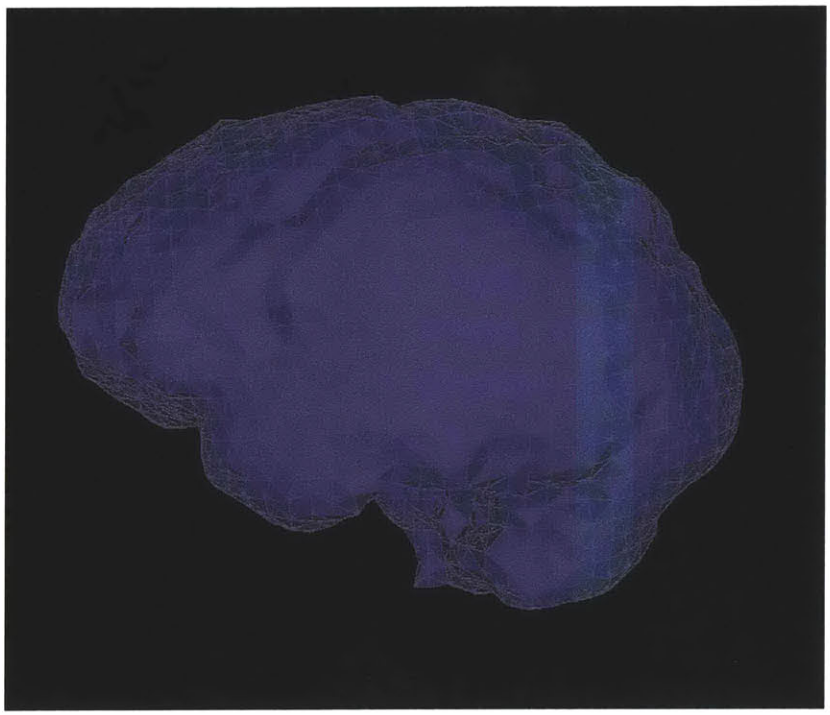

Figure 4-1: Surface boundary of the tetrahedral mesh.

Where σ_ν and d_ν are the conductivity and diffusion eigenvalues, respectively. The linear fit yields model parameters, $d_\varepsilon = 0.124 \pm 0.0545 \frac{\mu m}{ms}$, and $k = 0.844 \pm 0.0545 \frac{Ss}{mm^3}$.

4.3 Current Density Solution

After building the conductivity model, stimulation coordinates are used as input parameters, along with stimulation current amplitude, in solving the boundary-value problem for the current density distribution throughout the brain.

The problem at hand consists of solving for the electric field distribution over an asymmetric model with unknown charge distribution. This type of problem can be solved using Poisson's equation. The charge distributions and distribution of potential is determined by specifying the potential over the boundaries of the region [17]. This is described by Poisson's equation,

$$\nabla \cdot \sigma \nabla \Phi = -I_v.$$

Where σ is the conductivity tensor, Φ is the electric potential over the domain, and I_v is the source term indicating the current sources within the domain. The current sources for this problem are on the surface of the brain at the stimulation sites.

Assuming a piece-wise linear potential field, the solution to Poisson's equation can be approximated using the finite element method (FEM). The finite element method is a numerical technique for solving problems governed by partial differential equations [15]. FEM techniques use a discretized domain to solve for the physical field at the nodes in a mesh. In our case, the brain geometry is approximated by a collection of tetrahedral elements and the nodes are the intersections of the tetrahedral elements.

The solution is discretized over the nodes and is a piece-wise approximation of the physical field. The value inside the tetrahedral elements are recovered using the node values. The FEM solving software, SCIRun/BioPSE, was used to find the solution [22, 2].

The current magnitude, I_{mag}, is computed by taking the magnitude of the gradient of the electric potential,

$$I_{mag} = |\nabla \Phi|.$$

This current magnitude solution is the DECS stimulation map. Figure 4-2 shows the current magnitude solution imposed on intra-operative 3D-SPGR data. The solution was thresholded at 0.3% of the maximum value. A rainbow color scale is used; the purple regions indicate larger current magnitude values and the red regions are low current magnitude values.

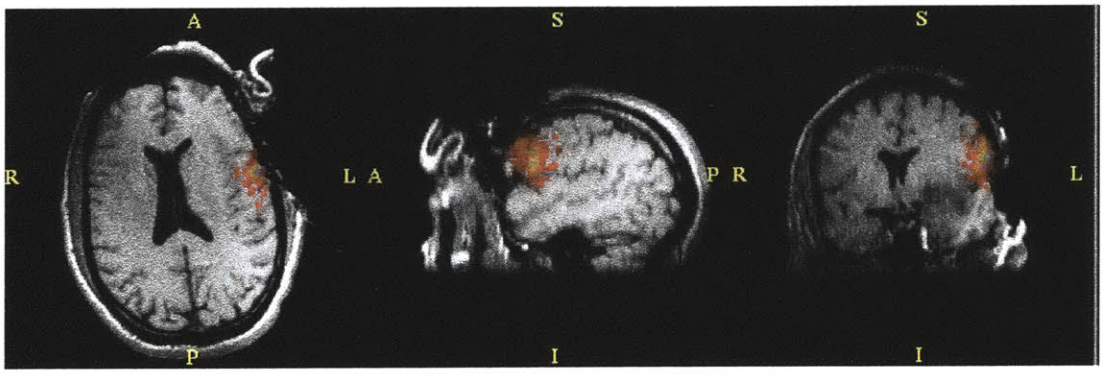

Figure 4-2: Current magnitude solution thresholded at 0.3% of the maximum current magnitude. A rainbow color scale is used where purple corresponds to the largest current magnitude and red is the lowest. The solution is imposed on intra-operative images at intersecting planes.

Chapter 5

Comparison of fMRI Activation and DECS Stimulation Maps

The 3D fMRI activation and DECS stimulation maps can now be compared to determine the level of agreement between the volumes. This comparison is quantified using the Dice similarity coefficient [4], which provides a quantitative measure of the degree of association between the two volumes. A Dice similarity coefficient (DSC) of 1.0 indicates that the two volumes are exactly the same; a DSC of 0.0 indicates that the volumes have no overlapping voxels. The DSC is defined as the number of intersecting voxels divided by the average number of voxels in each volume,

$$DSC = 2\frac{|V_1 \bigcap V_2|}{|V_1| + |V_2|}.$$

5.1 Functional Mapping: Region of Interest

In tumor resection, it is important to obtain a complete functional mapping near the craniotomy. fMRI and DECS methods help provide such a mapping. fMRI activation maps indicate that all activated voxels were responsible for performing the task. DECS stimulation maps indicate that somewhere within the stimulation region, eloquent cortex was activated and caused patient response. This complicates the comparison of the two volumes and it is not immediately obvious how to overcome

this problem. However, stimulated regions that evoke patient response indicate that eloquent tissue was stimulated and that region should be avoided during surgery.

5.1.1 fMRI Activation Map

The fMRI activation map is found by choosing paradigms that will activate regions within the region of interest - near the proposed craniotomy. fMRI activation protocols activate several regions in the brain; activation in this dataset is seen in language areas as well as in auditory, visual and motor areas. fMRI activation maps tell the surgeon that all voxels within activated regions were activated by the task performed. Using *a priori* knowledge, the surgeons observe the effects in the region of interest. fMRI activation maps provide confirmation of anatomy, and increased confidence in functional localization.

In this particular study, we are only interested in the regions near the craniotomy. For this case, Brocca's speech area is at risk of being damaged. Figure 5-1 shows two views of the fMRI activation volume; the orange region is the region of interest, and the purple regions are outside the region of interest.

5.1.2 DECS Stimulation Map

DECS functional mapping is obtained by choosing stimulation locations in the region of interest - the exposed cortex. The patient's observed response to stimulation establishes the stimulation mapping. Patient response to a particular stimulation site indicates that somewhere within the stimulation region eloquent cortex was activated causing the response. However, it is unknown exactly which cortical tissue within the stimulation region was responsible. This is quite different from the information that fMRI activation regions provide and therefore, there is an inherent inconsistency in comparing the two functional mapping methods.

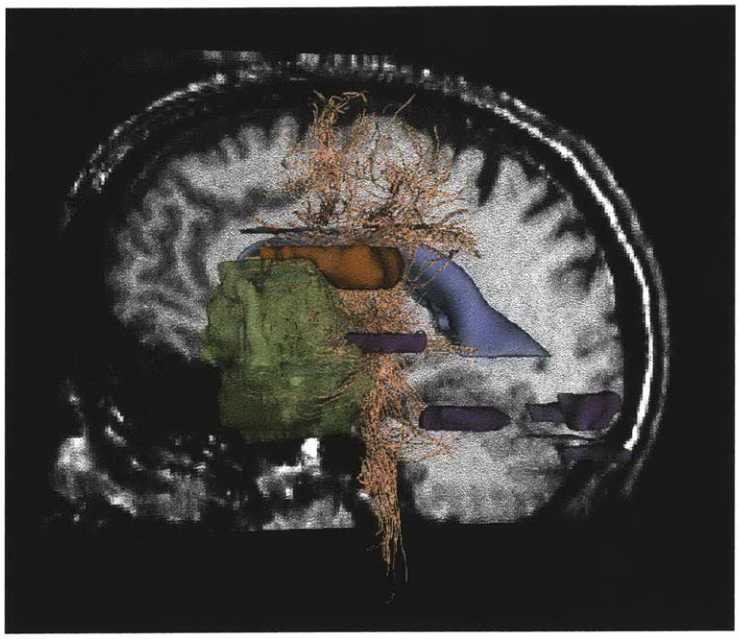

(a) Left view on sagittal pre-operative slice.

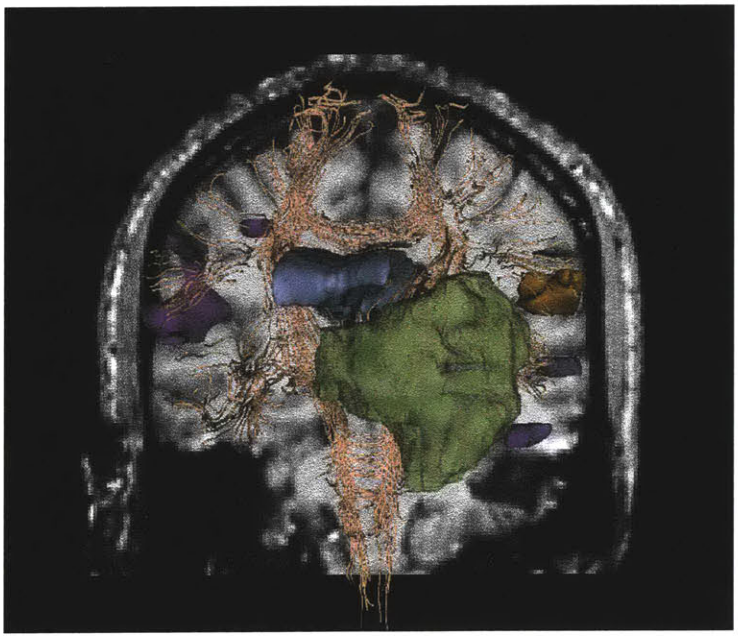

(b) Anterior view on coronal pre-operative slice .

Figure 5-1: fMRI activation in the region of interest (orange), and outside the region of interest (purple), tumor (green), ventricles (blue), white fiber tracts (yellow).

5.2 DECS Mapping Results

Seven sites were stimulated during the DECS intra-operative functional mapping procedures (see Figure 3-7 for stimulation sites). The mapping resulted in language inhibition at stimulation site number three. At this site the patient's language task was inhibited while the cortex was stimulated. The patient was asked to count from one to ten. When the cortex was stimulated, the patient stopped counting, and when the stimulation was removed the patient continued. This occurred at a current stimulation amplitude of $8mA$ and a frequency of $75Hz$. This information was used as input parameters in solving the boundary condition problem for current density distribution. The magnitude of the current density distribution makes up the DECS stimulation map.

For this study two electrode orientations were investigated: 1) Anterior-posterior (AP), and 2) Superior-inferior (SI). The two orientations produced differing results. Figure 5-2 shows the current density solutions for the two stimulator orientations. The stimulation sites are marked with two dark blue spheres indicating location and orientation of the bipolar stimulator. The DECS stimulation maps are shown in pink.

5.3 Comparison Results

In order to compare the fMRI activation and DECS stimulation maps, the DECS stimulation was thresholded. The threshold on current density that causes physiological effect is difficult to determine. Therefore, we thresholded the DECS stimulation map over the full range of current density values within the stimulation map. The Dice similarity coefficient was computed for each threshold. It is very likely that the threshold that causes physiological effect will be different from the threshold that maximizes the Dice similarity coefficient. This introduces bias into the DSC measure. Figure 5-3 shows a plot of DSC as a function of DECS activation map thresholds for each stimulator orientation. The maximum DSC for AP stimulator orientation is 0.1800 and occurs when the DECS stimulation map is thresholded at

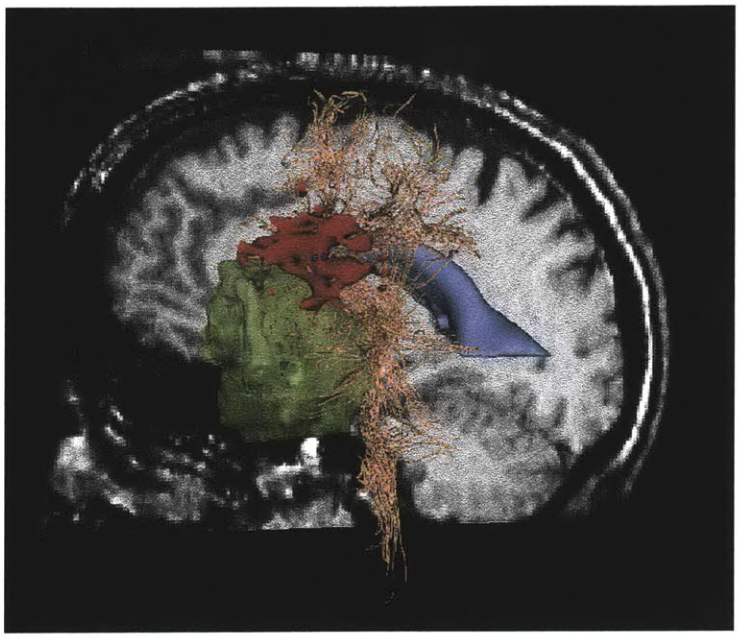

(a) AP stimulator orientation. Current density solution isosurface (dark pink) thresholded at $0.0024 mA/cm^3$.

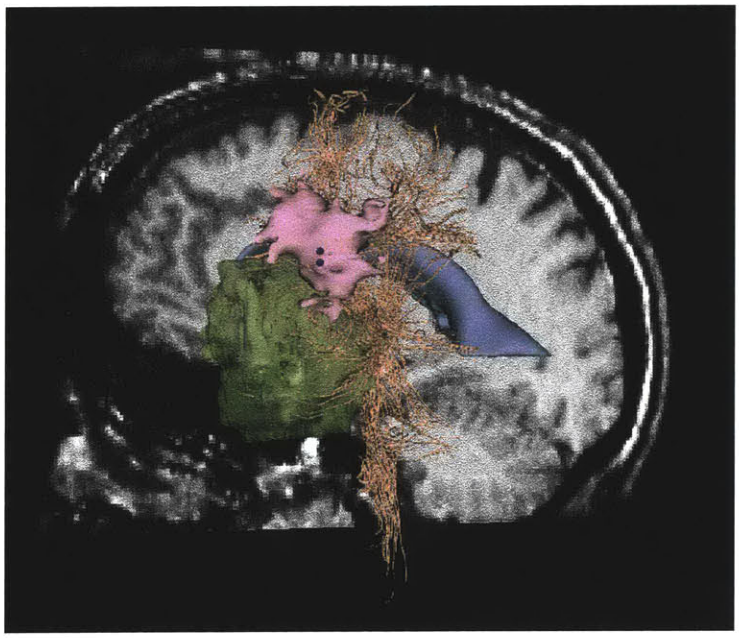

(b) SI stimulator orientation. Current density solution isosurface (light pink) thresholded at $0.0051 mA/cm^3$.

Figure 5-2: Comparison of current density solution (pink) for different stimulator orientations at stimulation site three (dark blue). Sagittal pre-operative slice, tumor (green), ventricles (blue) and white fiber tracts (yellow) are also shown.

$I_{mag} = 0.0024\frac{mA}{cm^3}$. The maximum DSC for SI stimulator orientation is 0.1747 and occurs when the DECS stimulation map is thresholded at $I_{mag} = 0.0051\frac{mA}{cm^3}$.

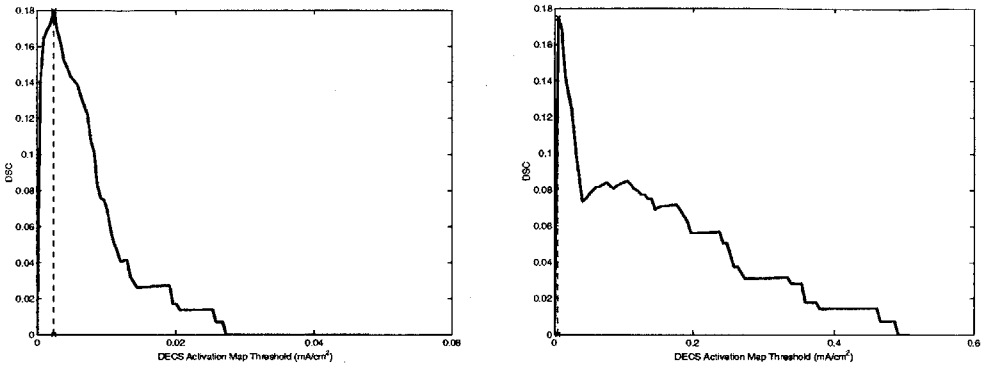

(a) AP DSC values as a function of DECS stimulation map threshold

(b) SI DSC values as a function of DECS stimulation map threshold

Figure 5-3: Comparison DSC values plots for different stimulator orientations.

Figure 5-4 shows the fMRI and DECS stimulation volumes for both AP and SI stimulator orientations. The DECS stimulation maps are thresholded at $I_{mag} = 0.0024\frac{mA}{cm^3}$ and $I_{mag} = 0.0051\frac{mA}{cm^3}$ for the AP and SI stimulator orientations, respectively. The stimulation sites are marked with two dark blue spheres indicating location and orientation of the bipolar stimulator. The DECS stimulation maps are shown in pink and the fMRI activation map for the region of interest is shown in orange. Figure 5-5 shows close-up views of the DECS stimulation map and fMRI activation map in the region of interest. Tables 5.1 and 5.2 lists the maximal DSC values for the current density solution at all seven stimulator positions for each orientation.

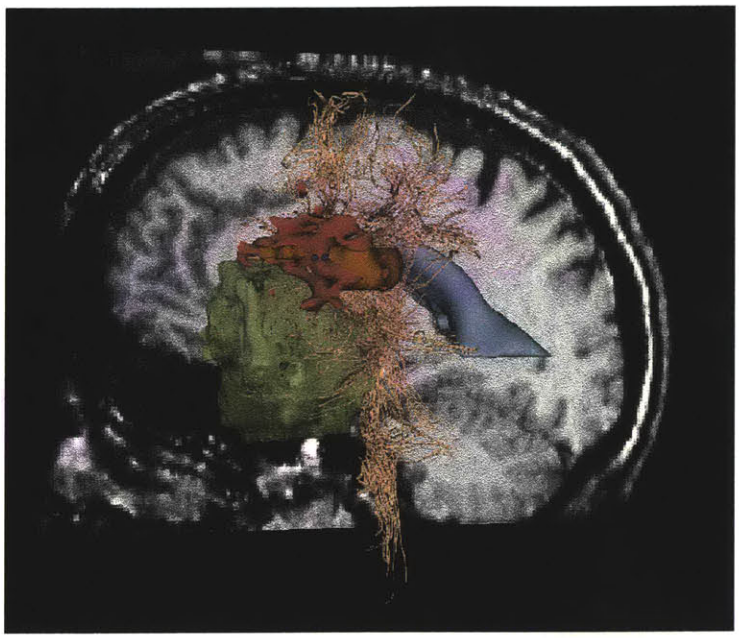

(a) AP stimulator orientation.

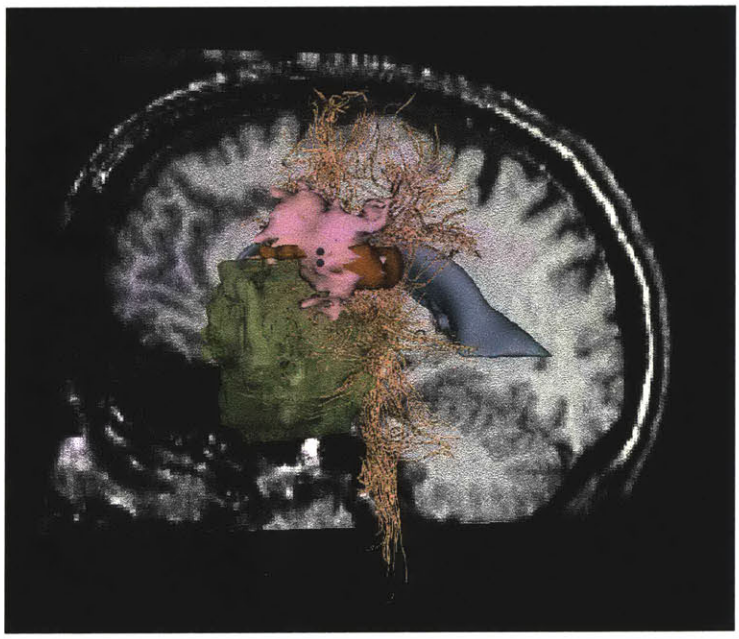

(b) SI stimulator orientation.

Figure 5-4: Comparison of current density solution (pink) and fMRI solution (orange) for different stimulator orientations at stimulation site three (dark blue). Models shown on sagittal pre-operative slice. The tumor (green), ventricles (blue) and white fiber tracts (yellow) are also shown.

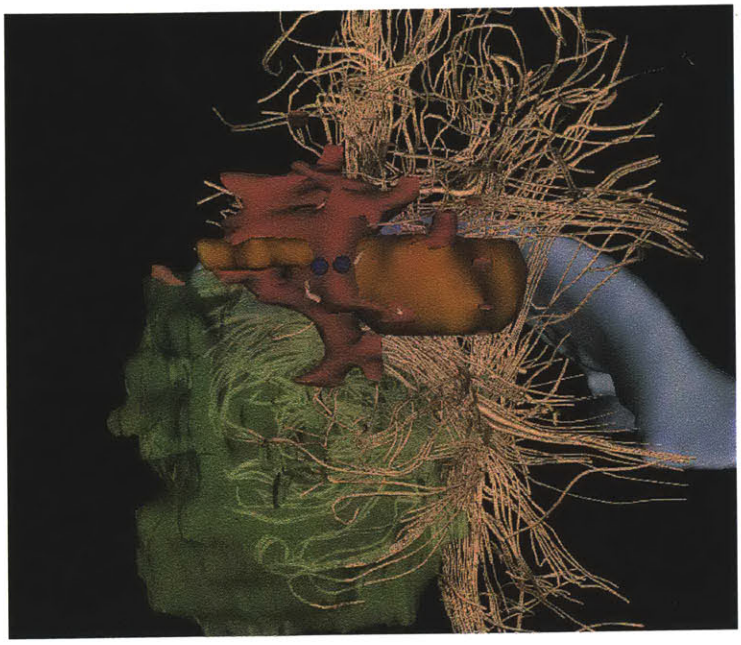

(a) AP stimulator orientation.

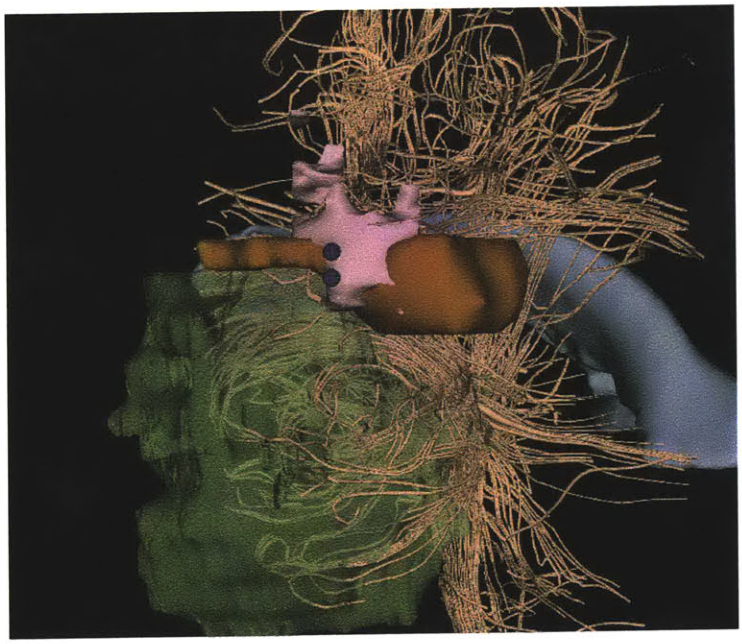

(b) SI stimulator orientation.

Figure 5-5: Zoomed in view of current density solution (pink) and fMRI solution (orange) for different stimulator orientations at stimulation site three (dark blue). Models shown on sagittal pre-operative slice. The tumor (green), ventricles (blue) and white fiber tracts (yellow) are also shown.

Table 5.1: Maximal DSC values for all electrodes when stimulator is in anterior-posterior orientation.

Stimulation Site	Maximal DSC
1	0.0547
2	0.0331
3	**0.1800**
4	0.0153
5	0.0
6	0.0015
7	0.0

Table 5.2: Maximum DSC values for all electrodes when stimulator is in superior-inferior orientation.

Stimulation Site	Maximum DSC
1	0.0533
2	0.0157
3	**0.1747**
4	0.0
5	0.0
6	0.0
7	0.0

5.4 Summary

The DECS stimulation and fMRI activation maps were compared using Dice similarity coefficients (DSC). The DSC provides a quantitative measure the of the degree of overlap between the two activation maps.

The fMRI activation map was defined within a region of interest around the craniotomy. The region of interest for this case was the Brocca speech area. The DECS stimulation map was generated based on the current density solution at stimulation site three. This is the only site where the patient's speech was inhibited due to stimulation. This stimulation site along with stimulation parameters, $8mA$ at $75Hz$, was used to generate the current density solution throughout the brain. This current density solution is the DECS stimulation map.

The DECS stimulation map at stimulation site three shows agreement with the fMRI activation map. The one stimulation site that evoked patient response during cortical mapping is the only site that shows agreement with the fMRI activation map. While stimulator orientation had an affect on the shape of the current density solutions, both orientations showed similar agreement with the fMRI activation map. Stimulation orientation during surgery is not normally considered. These results show that it does have an effect on patient response.

Chapter 6

Summary and Conclusions

6.1 System Overview

We introduce a method for quantitative comparison of fMRI and DECS functional mapping methods using patient-specific anisotropic conductivity models. We use existing technologies to achieve multi-modal image registration, and segmentation of brain, tumor and ventricles. We also use existing meshing technologies in order to find the electric field distribution using the finite element method. Figure 6-1 provides a system overview of our methods. Table 6.1 provides a summary of the time involved in each of these steps. The interaction time refers to the amount of time needed to set up the specifications of the action.

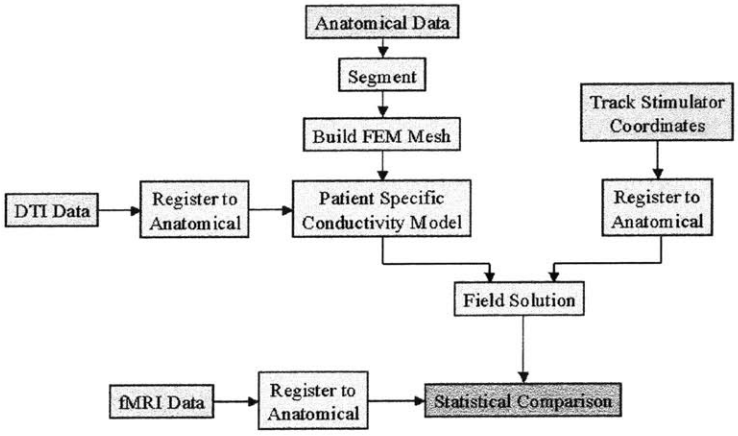

Figure 6-1: System overview block diagram.

Table 6.1: Summary of Time Involved

Action	Interaction Time	Computation Time
Manual Registration of all Data	Several hours	Several hours
Preparation for Automatic Segmentation	2 min	1 min
Automatic Segmentation (brain and ventricles)	5 min	2 min
Load Segmentation Results into Slicer	2 min	4 min
Manual Segmentation Correction in Slicer	30-60 min	10 min
Manual Tumor Segmentation	10-15 min	3 min
Tetrahedral Mesh Construction	30 min	2 min
FEM Solving	30 min	2 min

6.2 Discussion of Results

Localization of functional areas for surgical planning is of vital importance in successful tumor resection. fMRI has become a valuable source of information for functional mapping. Better understanding of how fMRI compares to cortical stimulation will lead to better understanding of functional mapping.

Our results show agreement between intra-operative cortical mapping results and fMRI activation results. fMRI paradigms were selected to activate regions of the brain within the region of interest. The DECS stimulation map is the magnitude of the current density solution due to cortical stimulation at site three with an amplitude of $8mA$ and a frequency of $75Hz$. The DECS stimulation maps show agreement with the fMRI activation map. The stimulation sites that did not evoke patient response do not show significant agreement with the fMRI activation map.

Stimulator orientation had an effect on the current density solution. The tracking device in the MRT does not currently have the ability to track stimulator orientation, but intra-operative cortical stimulation did show evidence that stimulator orientation had an affect on the patient's response. We simulated two different stimulation orientations. The two orientations had differing shapes in thresholded activation maps (see Figure 5-2). Additionally, when the stimulator was oriented anterior-posterior the threshold that produced the most agreement (largest DSC with the fMRI ac-

tivation map was 0.5% of the maximum. The threshold that produced the most agreement for the superior-inferior orientation was only 0.1% of its maximum current density magnitude. This indicates that the superior-inferior orientation had a larger effect on the patient's response. Unfortunately, we do not have a way to validate orientation effects with this dataset. However, while the two orientations showed a different shape in the current density isosurfaces, both solutions were still consistent with fMRI activation results.

Since cortical stimulation is considered the gold standard for intra-operative functional mapping, validation of fMRI is dependent on information obtained from surgery; there are several sources of error that can result. Tracking stimulation sites during surgery is a major source of error. While we are able to obtain coordinates from the stereotactic navigation probe, the probe is still tracking labeled tags on the cortical surface. These tags move around easily because the cortical surface must be continually flushed with saline solution. Also, the brain tends to shift after the craniotomy, and as time goes by, the brain can start to swell. Brain swelling can be caused by edema due to the tumor, increase in PCO_2, or gravity. Improvements to the tracking system need to be made. Tracking the stimulator as it stimulates rather than locating the tags with a separate tracker would be a great improvement. Additionally, it is important to track stimulator orientation.

More work needs to be done to improve the conductivity model. This includes non-rigid registration of intra-operative images to pre-operative images, and higher resolution DTI. At this point, the resolution of the tetrahedral mesh is limited by the resolution of the DTI data. Additionally, more surgical cases need to be investigated to perform a more comprehensive statistically study on how fMRI activation and DECS stimulation maps compare.

There is a substantial effort on the part of scientists and neurosurgeons to improve the techniques used to map tumor and functional area locations particularly by the usage of fMRI. Eventually, fMRI techniques will provide a valid non-invasive means for functional mapping and can be performed ahead of time.

6.3 Contributions

We have introduced a method for quantitatively comparing fMRI and intra-operative direct-electro cortical stimulation mapping. We have integrated existing technologies to help validate fMRI for pre-surgical functional mapping.

The DECS stimulation map was generated using a patient-specific anisotropic conductivity model of the brain. Using FEM solving methods, the current density throughout the brain can be found. The magnitude of this current density is the DECS stimulation map.

The DECS stimulation map is a 3D representation of cortical surface stimulation, providing volumetric information about how current travels through the brain. This gives a more complete cortical mapping in response to particular stimulation sites. Additionally, the 3D activation map can be quantitatively compared to the fMRI activation map. This quantitative comparison provides a quantitative measure of the degree of agreement between the two functional mapping methods.

We have provided a method to validate the utility of fMRI for pre-surgical planning. A more accurate localization of function areas will lead to less injury of eloquent brain matter during surgery and a more ambitious approach to tumor removal. Our results show initial agreement between fMRI and cortical stimulation. Moreover, we introduce a method for use in further statistical comparison of fMRI and cortical stimulation methods.

6.4 Perspectives and Future Work

Since the model will allow one to understand the brain conductances and field propagation of stimulation currents, it could make depth stimulation possible. With the use of two or more electrodes on the brain surface, one might be able to focus the field potentials to achieve stimulation at sulcul depths. This could lead to a more complete mapping of functional areas.

Additionally, incorporation of FEM field solving with patient specific anisotropic

conductivity models into the operating room could provide neurosurgeons with real time field solutions to cortical stimulation. This would provide them with more information when planning for tumor resection.

Appendix A

Abbreviations

Table A.1: Abbreviations

3D-SPGR	An inherently 3D gradient-echo MRI protocol that provides good anatomical contrast and resolution
AP	Anterior-Posterior
CMAP	Compound Muscle Action Potential
DECS	Direct-Electro Cortical Stimulation
DSC	Dice Similarity Coefficient
DTI	Diffusion Tensor Imaging
ECS	Electro-Cortical Stimulation
EEG	Electroencephalography
FEM	Finite Element Method
fMRI	functional Magnetic Resonance Imaging
GLM	General Linear Model
LSDI	Line Scen Diffusion Images
MEG	Magnetoencephalography
MRI	Magnetic Resonace Imaging
MRT	Magnetic Resonance Therapy
PE	Parameter Estimate
PET	Positron Emission Tomography
SCIRun/BIOPSE	Scientific Computing and Imaging field solving software Bioelectric Problem Solving Environment
SI	Superior-Inferior
SPM99	Statistical Parametric Mapping Software
T2-FSE	T2-weighted Fast Spin Echo
TMS	Transcranial Magnetic Stimulation

Bibliography

[1] A. Anwander, C.H. Wolters, M. Dumpelmann, and T. Knosche. Influence of realistic skull and white matter anisotropy on the inverse problem in eeg/meg-source localization. *Proceedings of the International Conference on Biomagnetism*, 2002.

[2] BioPSE: Problem Solving Environment for modeling, simulation, and visualization of bioelectric fields. Scientific Computing and Imaging Institute (SCI), http://software.sci.utah.edu/biopse.html, 2002.

[3] P.B. Black and M.R. Proctor. Minimally invasive surgery. scheduled to release March 2004.

[4] L.R. Dice. Measures of the amount of ecologic association between species. *Ecology*, 26(3):297–302, 1945.

[5] D.B. FitzGerald, G.R. Cosgrove, S. Ronner, and *et al.* Location of language in the cortex: a comparison between functional mr imaging and electrocortical stimulation. *American Journal for NR*, 18:1529–1539, 1997.

[6] K.J. Friston, P.J. Jezzard, and R. Turner. Analysis of functional MRI time-series. *Human Brain Mapping*, 1, 1994.

[7] D.T. Gering, A. Nabavi, and *et al.* An integrated visualization system for surgical planning and guidance using image fusion and an open mr. *Journal of Magnetic Resonance Imaging*, 13(6):967–975, 2001.

[8] H. Gudbjartsson, S.E. Maier, R.V. Mulkern, and *et al.* Line scan diffusion imaging. *Magn Reson Med*, 36(4):509–519, 1996.

[9] J. Haueisen, D.S. Tuch, C. Ramon, and *et al.* The influence of brain tissue anisotropy on human eeg and meg. *NeuroImage*, 15:159–166, 2002.

[10] D.L.G. Hill, A.D. Castelland Smith, A.Simmons, and *et al.* Sources of error in comparing functional magnetic resonance imaging and invasive electrophysiological recordings. *Journal of Neurosurgery*, 93:214–223, 2000.

[11] P. Jezzard, P.M. Matthews, and S.M. Smith, editors. *Functional MRI: and introduction to methods.* Oxford University Press, 2001.

[12] C.R. Jack Jr, R.M. Thompson, R.K. Butts, and *et al.* Sensory motor cortex: correlation of presurgical mapping with functional mr imaging and invasive cortical mapping. *Radiology*, 190:85–92, 1994.

[13] C.A. Kemper. Incorporation of diffusion tensor mri in non-rigid registration for image-guided neurosurgery. Master's thesis, Massachusetts Institute of Technology, 2003.

[14] T. Krings, M. Schreckenberger, V. Rohde, and *et al.* Metabolic and electrophysiological validation of functional mri. *Journal of Neurology, Neurosurgery, and Psychiatry*, 71:762–771, 2001.

[15] G.P. Nikishkov. *Introduction to the Finite Element Method.* University of Aizu, 2003.

[16] Radionics Ojemann Stimulator. http://www.radionics.com, 2003.

[17] C.R. Paul, K.W. Whites, and S.A. Nasar. *Introduction to Electromagnetic Fields.* McGraw Hill, 3 edition, 1998.

[18] A. Puce, R.T. Constable, M.L. Luby, and *et al.* Functional magnetic resonance imaging of sensory and motor cortx: comparison with electrophysiological localization. *Journal of Neurosurgery*, 83:262–270, 1995.

[19] J. Pujol, G. Conesa, J. Dues, and *et al.* Clinical application of functional magnetic resonance imaging in presurgical indentification of the central sulcus. *Journal of Neurosurgery*, 88:863–869, 1998.

[20] J. Schenk, F. Jolesz, and P. Roemer. Superconducting open-configuration of mr imaging system for image-guided therapy. *Radiology*, 195:805–814, 1995.

[21] M. Schulder, J.A. Maldjian, W.C. Liu, and *et al.* Function image guided surgery of intracranial tumors located in or near the sensorimotor cortex. *Journal Neurosurgery*, 89:412–418, 1998.

[22] SCIRun: A Scientific Computing Problem Solving Environment. Scientific Computing and Imaging Institute (SCI), http://software.sci.utah.edu/scirun.html, 2002.

[23] A.K. Sen and S. Torquato. Effective conductivity of anisotropic two-phase composite media. *Physics Review B*, pages 4504–4515, 1989.

[24] Slicer: Open-source software for visualization, registration, segmentation, and quantification of medical data. http://www.slicer.org, 2003.

[25] Statistical Parametric Mapping: Statistical process used to test hypotheses about neuroimaging data from SPECT/PET and fMRI. Wellcome Department of Imaging Neuroscience, http://www.fil.ion.ucl.ac.uk/spm/, 2003.

[26] I.F. Talos, L. O'Donnell, C.F. Westin, and *et al.* Diffusion tensor and functional mri fusion with anatomical mri for image-guided neurosurgery. *Sixth International Conference on Medical Image Computing and Computer-Assisted Intervention*, pages 407–415, 2003.

[27] S.J. Timoner. *Compact Representations for Fast Nonrigid Registration of Medical Images.* PhD thesis, Massachusetts Institute of Technology, 2003.

[28] D.S. Tuch, V.J. Wedeen, A. Dale, and *et al.* Conductivity tensor mapping of the human brain using diffusion tensor imaging. *Proceedings of the National Academy of Sciences*, 98(20):11697–11701, 2001.

[29] R. Van Uitert, D. Weinstein, and C.R. Johnson. Volume currents in forward and inverse magnetoencephalographic simulations using realistic head models. *Annals of Biomedical Engineering*, 31:21–31, 2003.

[30] I. Ulbert, G. Karmos, G. Heit, and E. Halgren. Early discrimination of coherent verus incoherent motion by multiunit synaptic activity in human putative mt+. *Human Brain Mapping*, 13:226–238, June 2001.

[31] T.F. Weiss. *Cellular Biophysics.* MIT Press, 1996.

[32] C. Westbrook and C. Caut. *MRI in Practice.* Blackwell Publishing, 1993.

[33] C.F. Westin, S.E. Maier, and *et al.* Processing and visualization for diffusion tensor mri. *Medical Imaging Analysis*, 6(2):93–108, 2002.

[34] F.Z. Yetkin, W.M. Mueller, G.L. Morris, and *et al.* Functional mr activation correlated with intraoperative corical mapping. *American Journal for NR*, 18:1311–1315, 1997.

[35] A. Yezzi, S. Kichenassamy, A. Kumar, and *et al.* A geometric snake model for segmentation of medical imagery. *IEEE Transactions on Medical Imaging*, 16:199–209, 1997.

[36] T.A. Yousry, A.G. Jassoy U.D. Schmid, and *et al.* Topography of the cortical motor hand area: prospective study with functional mr imaging and direct motor mapping at surgery. *Radiology*, 195:23–28, 1995.